aerospace

MDPI

Article

Compressive Behavior, Mechanical Properties and Energy Absorption of Al Honeycomb and Al Closed-Cell Foam: A Comparison

Alessandra Ceci, Girolamo Costanza * and Maria Elisa Tata

Industrial Engineering Department, University of Rome Tor Vergata, 00133 Rome, Italy; alessandra.ceci@uniroma2.it (A.C.); elisa.tata@uniroma2.it (M.E.T.)
* Correspondence: costanza@ing.uniroma2.it; Tel.: +39-06-72597185

Abstract: In this work, we focused on the characterization of closed-cell Al foams and aluminum honeycomb panels, in particular their energy absorption capacity under conditions of static compressive stress. Through experimental tests, the specific energy absorbed by different samples was evaluated: in the honeycomb panels the mechanical behavior was analyzed both for large assemblies and for structures with a reduced number of cells, and the effect of the number of cells was studied too. Furthermore, for larger structures, the specific energy absorbed was calculated from stress–strain compressive graphs. For the closed-cell Al foams, manufactured in the laboratory using the powder compaction method with different percentages of SiC and TiH_2 and characterized by different relative densities, the specific energy absorbed was evaluated too. The experimental results showed that the specific energy absorbed by the Al honeycomb was always higher than that of the different types of closed-cell foams. However, when selecting the material for each specific application, it is necessary to take into account numerous parameters such as the relative density, absorbed energy, peak stress, plateau stress, plateau extension, densification strain and so on. Consequently, the overall performance must be evaluated from time to time based on the type of application in which the best compromise between strength, stiffness and lightness can be achieved.

Keywords: closed-cell Al foams; Al honeycomb; static compression behavior; specific energy absorption; lightweight materials

check for updates

Academic Editor: Hyun-Ung Oh

Received: 9 December 2024
Revised: 31 December 2024
Accepted: 6 January 2025
Published: 8 January 2025

Citation: Ceci, A.; Costanza, G.; Tata, M.E. Compressive Behavior, Mechanical Properties and Energy Absorption of Al Honeycomb and Al Closed-Cell Foam: A Comparison. *Aerospace* **2025**, *12*, 32. https://doi.org/10.3390/aerospace12010032

1. Introduction

Cellular structures, such as foams, honeycombs and lattice structures, are increasingly being used in the transportation, aeronautical [1], naval [2], aerospace, high-performance vehicle [3,4] and bioengineering sectors where the stiffness/weight ratio plays a crucial role [5]. The honeycomb, in particular, finds application as an energy absorber thanks to its peculiar mechanical properties [6]. Many studies, in fact, have highlighted the importance of honeycomb in improving the impact resistance of structural components [7–9]. These structures, such as super hexagonal honeycombs [7] and foam-filled honeycomb panels, show higher energy absorption, specific energy absorption and volumetric energy absorption [7] capabilities in comparison with the traditional designs, showing advances in impact resistance and efficiency [6]. Metal foams are also increasingly used as energy absorbers due to their low density and energy absorption capacity. Guo et al. [10] proposed a novel efficient energy absorber with a necking-expansion of foam sandwich tubes. They found that the specific energy absorption of such an assembly is 68% higher than the circular metal tube under expansion deformation. Xu et al. [11] introduced a novel thin-walled structure based on an outer tube and three inner tubes as an energy absorber during the lateral compression process. The researchers demonstrated that the foam-filled system provides a better efficient impact force reduction and desired deformation mode compared to an empty system. A novel concept of anti-seismic device with high damping and energy dissipation capacity has been proposed by de La Peña et al. [12]. The damper is constituted by a dissipative aluminum foam structure with a high dissipative capacity when activated under compression. The preliminary results and numerical tests are encouraging, confirming the potential of the solution. Buvanesh et al. [13] analyzed the morphological properties of closed-cell Al foams, correlating compressing strength and energy absorption capacity with porosity size and morphology. Finally, metal foams' key parameters (cell size, relative density, strain rate, base metal and composite structures) affecting energy absorption in metal foams have been discussed by Costanza et al. in [14]. More in general, metal foams, made with various metals, such as aluminum, magnesium, iron, titanium, nickel, copper and their alloys, can be produced starting from molten metal or using the powder metallurgy technique, giving rise to closed- or open-cell structures with different applications according to the different densities. Several studies [15,16] have shown that the insertion of metal foams in structures such as tubes, sandwiches or more complex systems can significantly improve the energy absorption capacity, deformation modes and force reduction impact, making them of considerable interest in engineering application, for example, in impact resistance and improved seismic performance. Ryan et al. [17] analyzed the shielding performance of honeycomb cores and open-cell Al foams in dynamic impacts, highlighting the possibility of the replacement of the honeycomb with Al open-cell foams as a shielding on ISS modules.

Here, the experimental activity had the objective of calculating the specific energy absorbed by Al honeycomb structures and Al foams and comparing the results. The first phase of the experimental campaign involved the execution of static compression tests on honeycomb samples. From the compression tests it was possible to obtain the stress–strain curves, from which we calculated the specific absorbed energy. Furthermore, the goal was to analyze the mechanical behavior of structures with a reduced number of cells, starting from a single cell up to a structure with six cells, to establish a correlation between the variation in properties based on the number of cells. The second phase of the experimental campaign began with the manufacturing of closed-cell Al foams using the powder compaction method. Different foams were made by varying the amount of foaming agent (TiH_2) and stabilizing agent (SiC). After manufacturing, the foams produced were cut to be able to carry out static compression tests, in order to obtain, as for the honeycomb, the stress–strain diagram and, subsequently, calculate the specific absorbed energy. Finally, a comparison was made between honeycomb and closed-cell foams in terms of the specific absorbed energy.

2. Materials and Methods

2.1. Honeycomb

The static compression tests on the aluminum honeycomb were carried out on 4 samples (see Figure 1) whose dimensions are shown in Table 1, and which were extrapolated from a single panel of aluminum honeycomb with hexagonal cells. The tests were conducted with a constant crosshead speed of 5 mm/min and were stopped at a strain of about 80%.

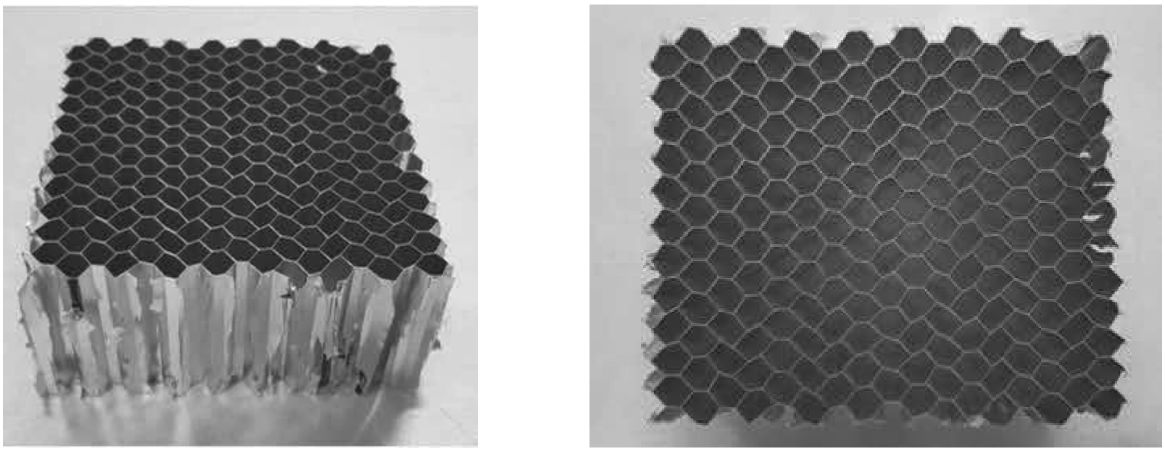

(a) (b)

Figure 1. (**a**) Side view and (**b**) top view of the Al honeycomb sample.

Table 1. Geometrical features of Al honeycomb specimens.

	Base Area [mm^2]	Height [mm]
Specimen 1	1091	50
Specimen 2	1185	50
Specimen 3	1215	50
Specimen 4	1496	50

As can be observed from Figure 1, due to the cutting made on the honeycomb panel to obtain the various specimens, there are defects on the edges. In fact, the outermost cells sometimes appear distorted and non-regular compared to the original hexagonal shape.

In addition to static compression tests on samples with a high number of cells, the strength of the material at increasing numbers of cells was evaluated too. The tests were carried out starting from a single cell up to six cells (Figure 2), increasing the number of cells by one unit each time.

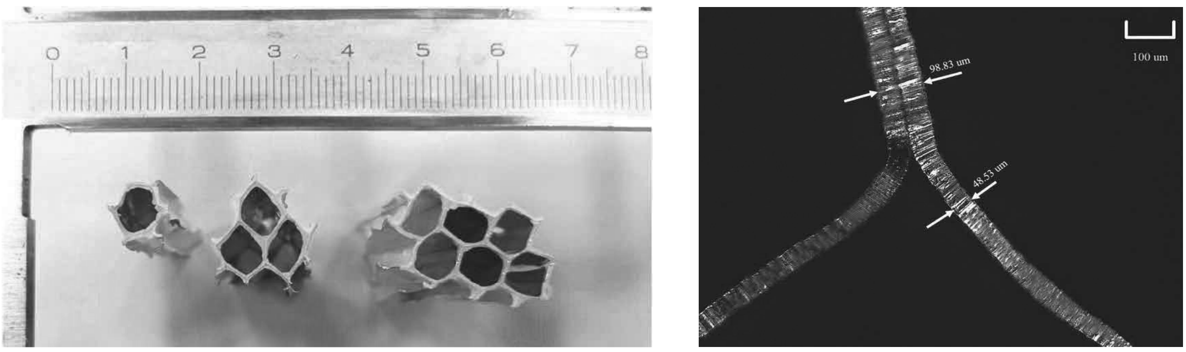

(a) (b)

Figure 2. (**a**) Hexagonal cell of Al honeycomb: 1 cell, 3 cells, 6 cells. (**b**) Light microscope micrograph with hexagonal cell wall thickness measurements.

2.2. Metal Foams

The technique adopted in the laboratory for the production of the Al foams used for the compression test was the compacted powders melting technique, described in detail in previous works [18,19]. For the production of aluminum foams, titanium hydride (TiH_2)

was used as a blowing agent, whose decomposition start temperature (400 °C) adapts well to the melting temperature of aluminum (660 °C); silicon carbide (SiC) powders were used as a stabilizing agent. Aluminum (powders) was the complement of 100.

Table 2 summarizes the main characteristics of the aforementioned powders. Based on a study conducted previously [19], it was decided to experimentally analyze the static compression behavior of six different compositions:

- 0.1% TiH_2–2.8% SiC;
- 0.1% TiH_2–6.0% SiC;
- 0.2% TiH_2–2.8% SiC;
- 0.2% TiH_2–6.0% SiC;
- 0.4% TiH_2–2.8% SiC;
- 0.4% TiH_2–6.0% SiC.

Table 2. Features of the powders employed for the manufacturing of the closed-cell Al foams.

Al Powders	
Maximum size	45 µm
Average size	40 µm
Melting temperature	660 °C
Density	2.7 g/cm^3
Purity	99.5%
Titanium Hydride Powders	
Ti	95% wt min
H	3.8% wt min
N	0.3% wt min
Maximum size	63 µm
Average size	5 ± 1 µm
Silicon carbide Powders	
Maximum size	37 µm

Powder mixing is crucial in the preparation of the precursor, because only a homogeneous distribution of the components ensures good quality, standardized and regular porosity to the foam. To mix the powders, a plastic container was used, mounted eccentrically on a rotative axis. The mixing time, which guarantees sufficient homogeneity of the mixture, for weights not exceeding 30 g, is 10 min. The type of compression used to obtain the precursor is cold (room temperature) uniaxial and guarantees the crushing of the oxide layer present in the Al powders when the compaction pressure applied is at least 200 MPa. The precursor, obtained from pressing, is successively introduced inside a stainless steel crucible into the oven, containing two precursors placed side by side. The crucible acts as a mold for the precursors which, in the liquid phase upon foaming, take on their shape. The crucible is inserted inside the oven maintained at a temperature of 700 °C. After 4–5 min (depending on the geometry and the size), the foaming process starts. The phenomenon can be divided into the following steps: a first phase in which growth is slow with the formation of small bubbles on the surface of the still solid precursor, then a rapid increase in volume of the liquid metal for about 20 s. Once maximum growth has been reached, the crucible containing the foam is removed from the oven and immersed in water to make it solidify and fix at room temperature the shape obtained at maximum growth (Figure 3a). The foams produced with the procedure just described have a rather rough external shape

(Figure 3a). To obtain specimens that could be used in compression tests, it was necessary to remove the imperfections and make cuts to obtain parallel sides in order to carry out the compression tests (Figure 3b).

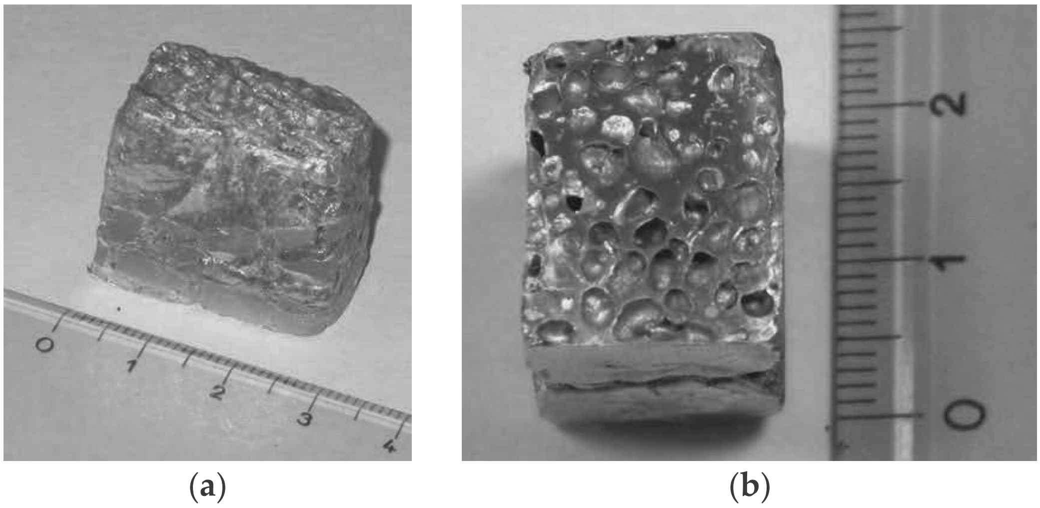

Figure 3. (**a**) Al foams manufactured with the powder compaction method. (**b**) Cross-section view of the Al manufactured foams after cutting.

The analyzed Al foam specimens had the geometric characteristics shown in Table 3.

Table 3. Geometrical features of Al foam samples.

Composition	Specimen n	Initial Section [mm^2]	Initial Heigth [mm]	Volume [cm^3]
0.1% TiH_2–2.8% SiC	1	410.0	20.0	8.2
	2	412.7	19.1	7.9
0.1% TiH_2–6.0% SiC	1	432.7	17.8	7.7
	2	422.0	20.1	8.5
0.2% TiH_2–2.8% SiC	1	434.0	22.3	9.7
	2	437.1	22.3	9.7
0.2% TiH_2–6.0% SiC	1	429.3	23.0	9.9
	2	431.5	22.8	9.8
0.4% TiH_2–2.8% SiC	1	429.7	23.1	9.7
	2	430.3	22.9	9.8
0.4% TiH_2–6.0% SiC	1	396.3	25.8	10.2
	2	402.6	25.0	10.1

3. Experimental Results

3.1. Honeycomb

Below is reported the image of a honeycomb sample positioned between the plates of the compression machine in an initial step of the test (Figure 4a) and the same specimen at the end of the compression (Figure 4b).

(**a**)

(**b**)

Figure 4. (**a**) Compression test on Al honeycomb. (**b**) Al honeycomb sample at the end of the static compression test.

Except for the edges of the specimen, during compression the deformation of the internal hexagonal cells occurred uniformly, without slipping; the plastic collapse of the walls of the hexagonal structure gave rise to honeycomb structures superimposed on each other, as can be seen in Figure 4b.

Figure 5 shows the comparison of the stress–strain diagrams for the four examined samples. As evidenced from the graph, a high repeatability of the compressive behavior was found in terms of peak stress, plateau stress and total strain before final densification.

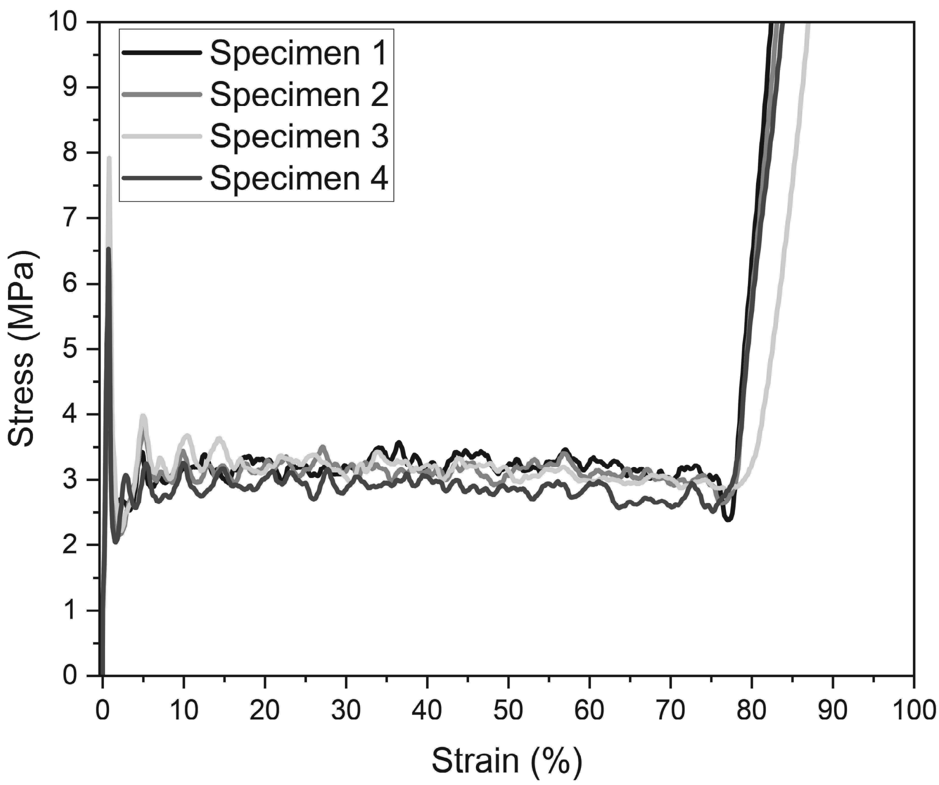

Figure 5. Stress–strain comparison curves of the four considered honeycombs.

Compression tests were also carried out on Al honeycomb samples with an increasing number of cells, from one to six. The load–strain diagrams are reported in Figure 6.

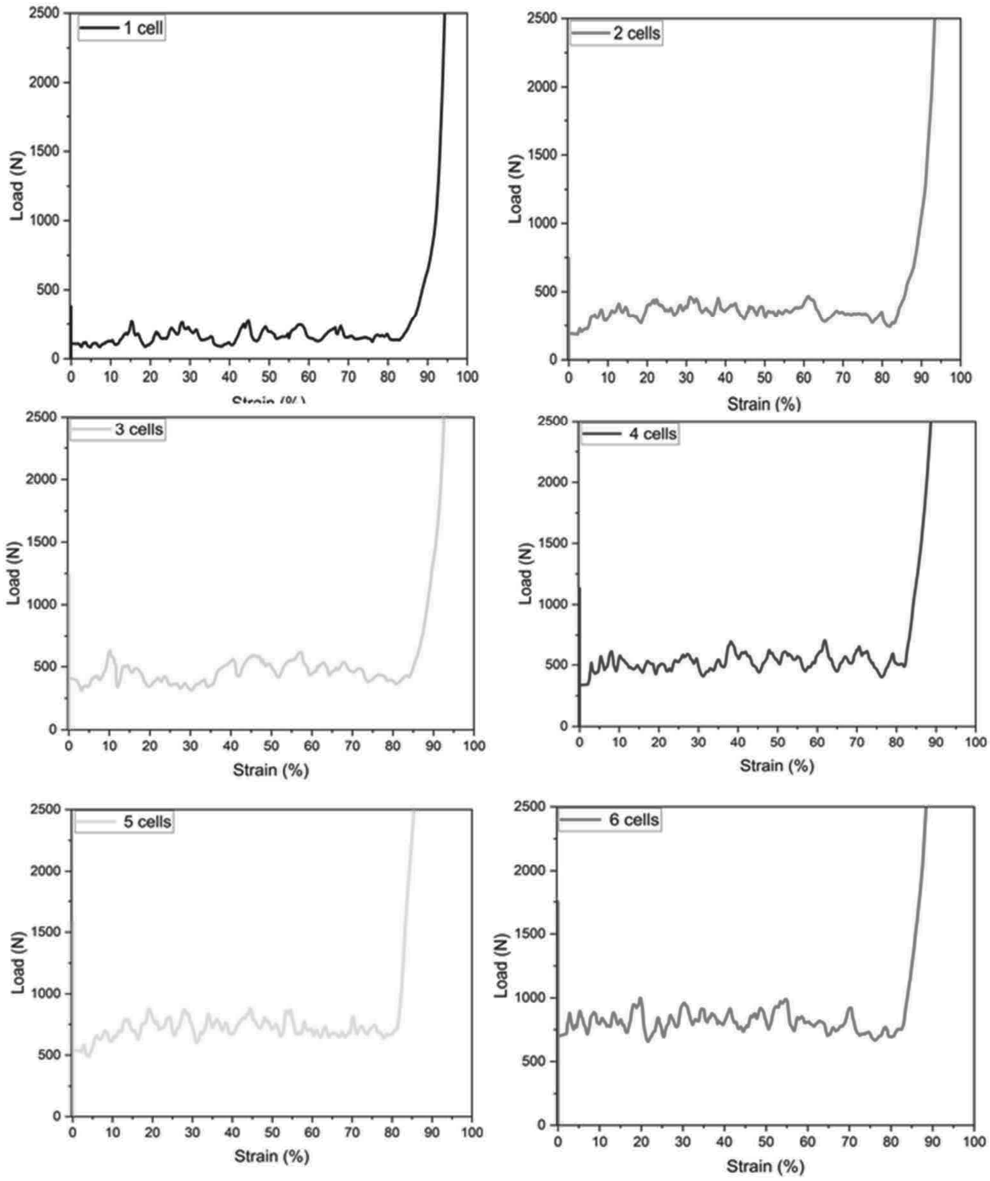

Figure 6. Load–strain curves of the Al honeycomb cells (1 to 6 cells).

3.2. Metal Foams

Figure 7 shows the different steps of the compression test of Al metal foams and Figure 8 shows the corresponding stress–strain diagrams. After an initial linear stage, an extended plateau with approximately constant stress follows, during which the deformation occurs of the walls of the foams and, finally, there is a fast increase in stress due to the final densification.

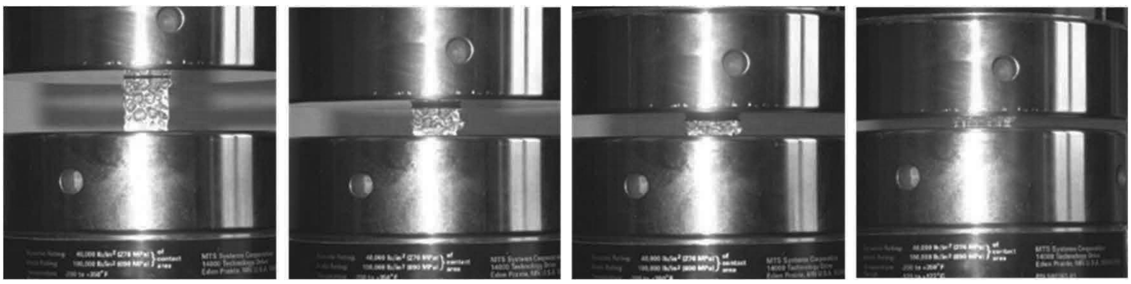

Figure 7. Successive compression steps of Al foam specimen.

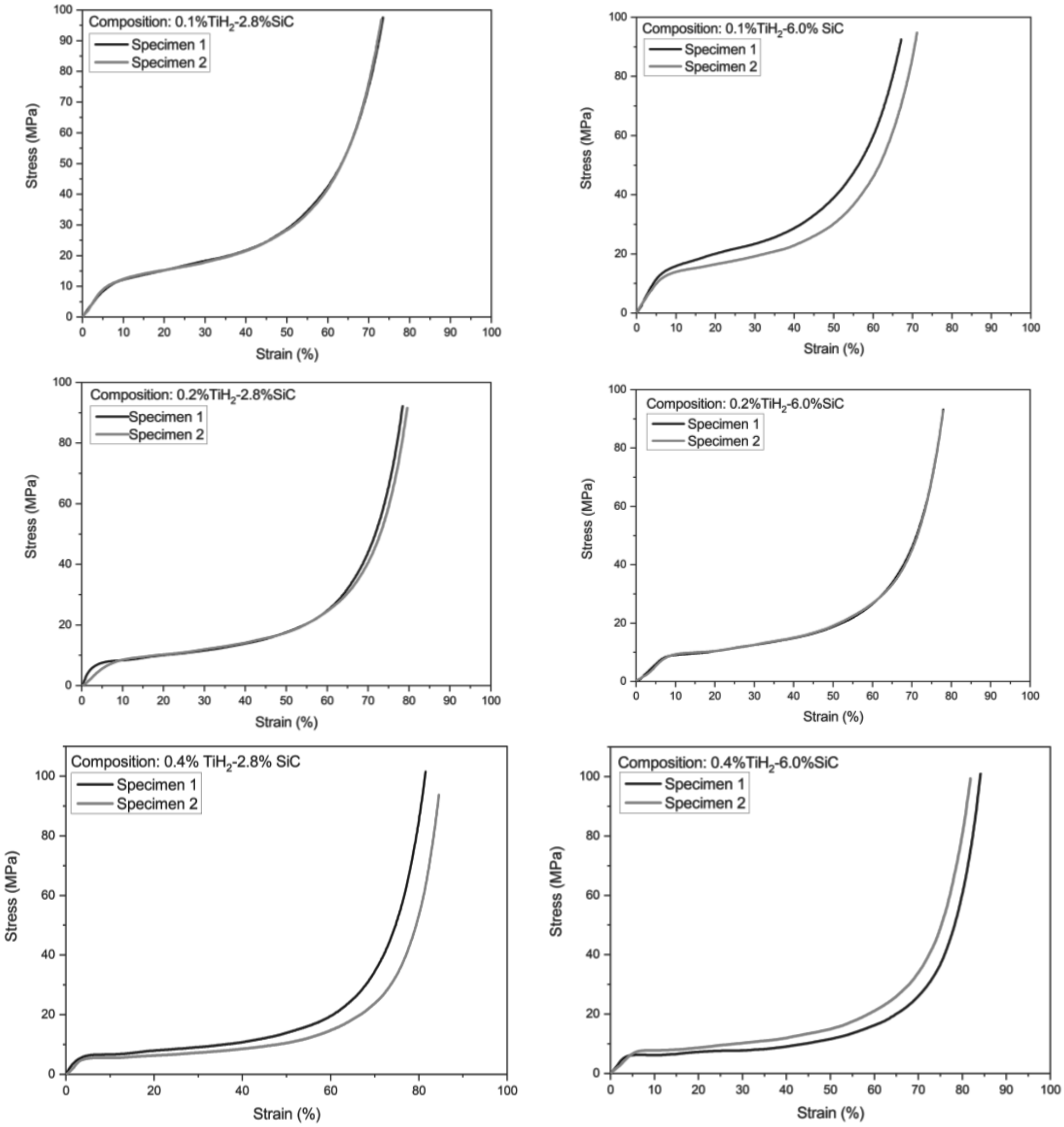

Figure 8. Stress–strain diagrams for the manufactured Al foams.

4. Discussion

4.1. Honeycomb

Comparing the data obtained from the four compression tests carried out on the honeycomb specimens (Figure 5), it is evident that with the same (or almost equal) base area and height of the specimen, the behavior of the aluminum honeycomb was approximately equivalent. A good repeatability of the data was observed in the four tests; in fact, the values of initial peak stress, σ_{pk}, and plateau stress, σ_{pl}, remained at an almost constant value, as reported in Table 4, where the main parameters obtained from the compression curves are reported. The subscript pk refers to the point at which the initial peak of maximum stress and the corresponding deformation ε_{pk} occurs, while the subscript pl refers to the plateau. The σ_{pl} was calculated as the average value assumed at a stress of 0.8% to 80% of strain.

Table 4. Mechanical features of Al honeycomb samples.

	ε_{pk} %	σ_{pk} [MPa]	σ_{pl} [MPa]
Specimen 1	0.8	6.8	3.2
Specimen 2	0.8	6.4	3.1
Specimen 3	0.8	7.9	3.1
Specimen 4	0.8	6.2	2.8

The following graph (Figure 9) shows the trends in specific energy absorption as a function of the deformation experienced by the Al honeycomb during compression. The specific absorbed energy values were calculated with the following formula:

$$E_{specific} = v\int_0^{\overline{\varepsilon}} \sigma d\varepsilon \quad (1)$$

where $v = 0.018\ \frac{m^3}{kg}$ is the specific volume, the reciprocal of density, as derived from the technical specification equivalent at 56 $\frac{kg}{m^3}$; and $\overline{\varepsilon}$ is the considered strain (from 10% to 80% at increments of 10%) just before the final densification.

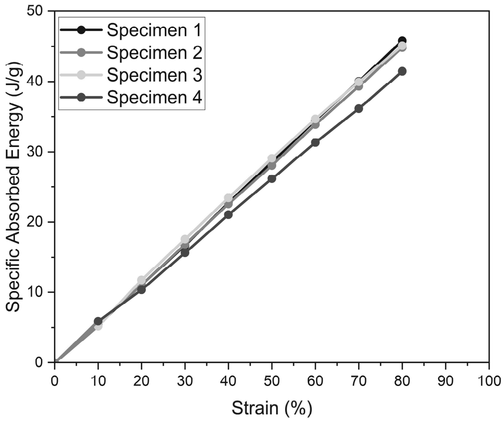

Figure 9. Specific absorbed energy–strain diagram for static compression on Al honeycomb.

Table 5 shows the values of specific energy absorbed for the various Al honeycomb specimens corresponding to different deformation values.

Table 5. Specific absorbed energy for Al honeycomb specimens.

Strain %	Specific Absorbed Energy [J/g]			
	Specimen 1	**Specimen 2**	**Specimen 3**	**Specimen 4**
10	5.4	5.5	5.2	5.9
20	11.0	11.0	11.7	10.3
30	16.7	16.8	17.6	15.6
40	22.7	22.6	23.4	21.0
50	28.5	28.0	29.0	26.1
60	34.5	33.9	34.6	31.3
70	40.0	39.3	39.9	36.1
80	45.8	44.8	45.1	41.4

By analyzing the specific energy absorption (Figure 9 and Table 5), it can be observed that the behavior of the four specimens was almost similar. For a deformation of 80%, there was an average value of specific absorbed energy of approximately 44 J/g. This result provides further confirmation of the good repeatability of the experimental data.

For the static compression tests performed on structures with a reduced number of cells, Table 6 shows the values of the maximum load and the plateau load.

Table 6. Main parameters for Al honeycomb compression tests at increasing number of cells.

Number of Cells	Maximum Load [N]	Plateau Load [N]
1	363	142
2	736	337
3	1183	385
4	1031	520
5	1634	639
6	1738	793

Finally, the peak stress (σ_{pk}), corresponding to the point at which the maximum stress occurs, and the plateau stress (σ_{pl}), as a function of the deformation of the samples with an increasing number of cells from one to six, were calculated and are reported in Table 7. The total area of the hexagon was considered the area, without the cavities as such (same consideration as for the tests on large samples).

Table 7. Peak stress values (σ_{pk}) and plateau stress values (σ_{pl}) for samples with increasing number of cells.

Number of Cells	σ_{pk} [MPa]	σ_{pl} [MPa]
1	8.8	3.4
2	8.9	4.1
3	9.5	3.1
4	6.2	3.1
5	7.9	3.1
6	7.0	3.1

Concerning the tests performed on individual honeycomb cells, increasing values of the maximum load and the plateau load can be observed as the number of cells increases (Table 6). As evidenced by the increasing values of both the maximum load and the plateau load, these highlight how the strength of the aluminum honeycomb increased as the number of cells increased and, therefore, the surface on which the load is distributed increases. For the values obtained by dividing the load by the area, they appear to be almost constant and independent of the number of cells. The average obtained average value equaled 8 MPa for σ_{pk} and 3.3 MPa for σ_{pl}.

4.2. Al Foams

The following graph (Figure 10) shows the comparison of compressive tests performed on Al foams with different compositions. The individual curves were obtained as averages of the trends of the two specimens used for the various compositions. Furthermore, as a comparison, the yield value at 0.2% is reported for an EN AW-1070 Aluminum alloy (Al content $\geq$ 99.70%) of 50 MPa (according to EN 485-2: 2016).

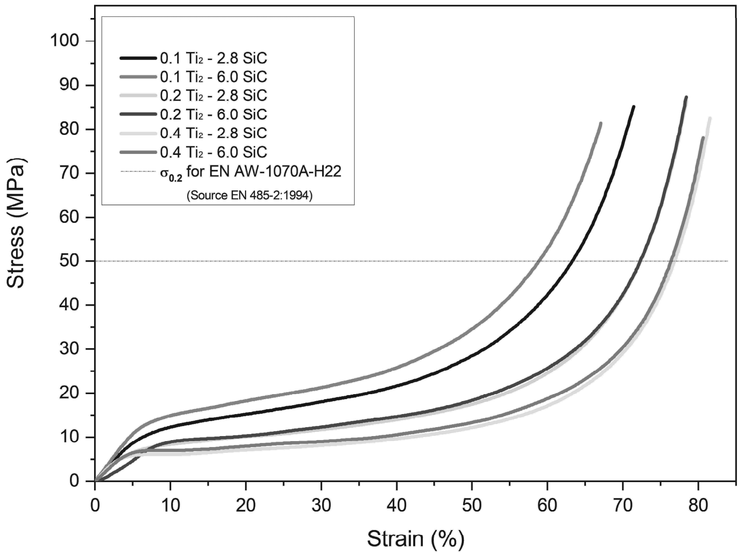

Figure 10. Stress–strain compression for Al foams.

The following graph (Figure 11) shows the trends of specific energy absorption as a function of the deformation undergone by the foams. This specific energy value was calculated with the Formula (1) where v is the specific volume, which is the reciprocal of the density shown in Table 8.

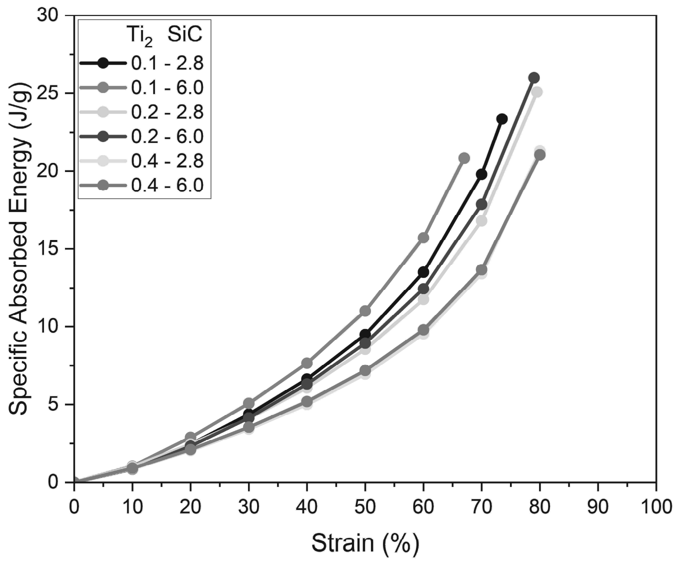

Figure 11. Specific absorbed energy–strain diagram for Al foams.

Table 8. Mechanical characteristics of Al foams.

Composition	ρ [g/cm^3]	ρ/ρ_0	E [MPa]	E/E_0 [%]	σ_{el} [MPa]	Growth %
0.1% TiH_2–2.8% SiC	0.872	0.321	193.2	0.284	8.0	186.9
0.1% TiH_2–6.0% SiC	0.901	0.331	246.2	0.362	11.0	187.0
0.2% TiH_2–2.8% SiC	0.640	0.236	267.5	0.393	6.7	248.0
0.2% TiH_2–6.0% SiC	0.636	0.233	143.8	0.211	6.7	293.8
0.4% TiH_2–2.8% SiC	0.558	0.205	211.7	0.311	4.5	387.8
0.4% TiH_2–6,0% SiC	0.595	0.218	170.5	0.251	5.4	390.0

Table 8 shows the main characteristics obtained for the various compositions of Al foams analyzed in terms of their strength, density and percentage growth. ρ expresses the average density of the single foam composition, while ρ_0 indicates the density of the massive material ($\rho_0 \approx 2.72$ g/cm^3). E is the average Young's modulus identified for the various compositions, calculated through the slope of the linear section of the stress–strain curve. E_0 is the Young's modulus of pure aluminum, equal to approximately 68,000 MPa. σ_{el} is the stress at the end of the elastic linear section. Finally, growth or expansion is defined as (H_final-H_initial)/H_initial, where H_initial is the height of the unfoamed precursor, equal to 8.0 mm.

Table 9 shows the absorbed specific energy values for all the Al foam specimens.

Table 9. Specific absorbed energy for the manufactured Al foams.

Strain %	Specific Absorbed Energy [J/g]					
	0.1–2.8%	**0.1–6.0%**	**0.2–2.8%**	**0.2–6.0%**	**0.4–2.8%**	**0.4–6.0%**
10	0.9	1.0	1.0	0.8	0.9	0.9
20	2.4	2.9	2.4	2.3	2.0	2.1
30	4.4	5.1	4.1	4.1	3.4	3.5
40	6.6	7.6	6.1	6.3	5.0	5.2
50	9.5	11.0	8.5	8.9	6.9	7.2
60	13.5	15.7	11.7	12.4	9.5	9.8
70	19.8	20.8	16.8	17.9	13.4	13.7

For closed-cell Al foams, from Figure 10 it is evident that a good repeatability of the results was achieved. In particular, it can be noted that the foams with 0.1% TiH_2 were those with the highest plateau stress; the 0.2% TiH_2 foams presented a lower plateau stress than the previous ones. Finally, foams with 0.4% TiH_2 showed the lowest plateau stress and the greatest deformations overall. With regard to the deformations achieved, the order was just the opposite. By analyzing the specific energy absorption (Table 9), it can be noted that for deformations of 50%, the 0.1% TiH_2 foams absorbed between 12% (for the composition with 0.2% TiH_2) and 38%, with more energy for the composition with 0.4% TiH_2. These differences increased at deformations of 60% by up to 26% and 60%, respectively.

5. Comparison of Results

Comparing the specific energy absorbed by the Al honeycomb and the aluminum foams, it is evident that the honeycomb had higher values for the same deformation compared to the foams. Table 10 shows the comparison between Al honeycomb specimen 1 (Figure 8 and Table 5) and the Al foam with 0.1% TiH_2–6.0% SiC (Figure 10 and Table 9), which appears to have, at each considered strain, the highest specific energy absorbed. The maximum considered strain was 70%, the maximum achievable strain for both considered materials.

Table 10. Specific absorbed energy comparison.

	Specific Absorbed Energy [J/g]	
Strain %	**Al Honeycomb Specimen 1**	**Al Foam 0.1% TiH_2–6.0% SiC**
10	5.4	1.0
20	11.0	2.9
30	16.7	5.1
40	22.7	7.6
50	28.5	11.0
60	34.5	15.7
70	40.0	20.8

The results of the preliminary comparison compressive tests showed that, under the same applied strain, Al foams exhibit a lower specific absorbed energy. In the comparison, Al honeycomb showed a nearly homogeneous plateau stress at around 3.3 Mpa, while for Al foams the plateau stress ranged from 8 to 20 MPa, depending on the composition of the powders, with particular reference to the TiH_2 amount. The stress–strain trend was similar for both materials; however, the difference in the final specific absorbed energy can be ascribed to the great difference in density between the materials, with a much higher density for closed-cell Al foams in comparison with a lightweight honeycomb.

6. Conclusions

In this work, static compression tests were carried out on Al honeycomb specimens and closed-cell aluminum foams with the aim of investigating the mechanical behavior and calculating the specific energy absorbed during these tests.

It was highlighted that the data obtained from the four tests carried out on the honeycomb were nearly equivalent and, therefore, the results showed good repeatability. The values of the initial peak stress and the plateau stress remained at an almost constant value, equal to 6.8 MPa and 3 Mpa, respectively, and the specific absorbed energy also exhibited approximately similar values (for a deformation of 50% of 28 J/g). We analyzed the behavior of the individual cells to understand how the number of cells influenced the behavior of the material. From the study of specimens with a reduced number of cells, it was evident that the peak stress and plateau stress values took on an approximately constant value, regardless of the number of cells, equal to 8 MPa and 3.3 Mpa, respectively.

In terms of the Al foams, those with 0.1% TiH_2 had a plateau at the highest stress levels; 0.4% TiH_2 foams had the lowest plateau stress values. Furthermore, for the same deformation, the 0.1% TiH_2–6.0% SiC foams had a greater specific absorbed energy than the others, and this phenomenon was more evident at increasing levels of deformation. This fact can be ascribable to the greater stress at which the plateau occurs in the case of the foam with 0.1% TiH_2.

The following conclusions were drawn:

(1) From the comparison in Table 10, it can be observed that for a strain equal to 50% the honeycomb had a value of specific absorbed energy approximately 160% higher than the foam with 0.1% TiH_2–6.0% SiC.
(2) Stresses were much higher in Al foams than honeycombs in the compression curves.
(3) Both of the analyzed structures are well suited for applications in which weight reduction plays a fundamental role. Consequently, it must be considered that the

selection of the appropriate material depends on the type of application and the project specifications.

(4) The foam's properties, such as its compressive strength and energy absorption, are particularly interesting in structural components for lightweight and high-strength applications, especially in aerospace transportations. Even between the same type of material, such as foams, it should be underlined that each characteristic must be related to the specific application. In fact, for example, despite having greater energy absorption, the foam with 0.1% TiH_2 is less suitable in the event of a crash as the higher plateau value would induce greater stress on the structure.

Author Contributions: Conceptualization, A.C., G.C. and M.E.T.; methodology, A.C., G.C. and M.E.T.; formal analysis, A.C., G.C. and M.E.T.; investigation, A.C., G.C. and M.E.T.; data curation, A.C., G.C. and M.E.T.; writing—original draft preparation, A.C., G.C. and M.E.T.; writing—review and editing, A.C., G.C. and M.E.T. All authors have read and agreed to the published version of the manuscript.

Funding: This research received no external funding.

Data Availability Statement: The data used to support the findings of this study are available from the corresponding author upon request.

Acknowledgments: The authors are grateful to Pieri Plini and Benedetto Iacovone for the technical assistance in sample manufacturing and experiments.

Conflicts of Interest: The authors declare no conflicts of interest.

References

1. Ganilova, O.A.; Cartmell, M.P.; Kiley, A. Experimental Investigation of the Thermoelastic Performance of an Aerospace Aluminium Honeycomb Composite Panel. *Compos. Struct.* **2021**, *257*, 113159. [CrossRef]
2. Liu, K.; Zong, S.; Li, Y.; Wang, Z.; Hu, Z.; Wang, Z. Structural Response of the U-Type Corrugated Core Sandwich Panel Used in Ship Structures under the Lateral Quasi-Static Compression Load. *Mar. Struct.* **2022**, *84*, 103198. [CrossRef]
3. Savage, G. Development of Penetration Resistance in the Survival Cell of a Formula 1 Racing Car. *Eng. Fail. Anal.* **2010**, *17*, 116–127. [CrossRef]
4. Faculty of Mechanical and Aerospace Engineering, Bandung Institute of Technology, Indonesia; Komara, A.I.; Bandung Polytechnic for Manufacturing, Indonesia; Budiwantoro, B.; Setiawan, R. Cellular Structure Design and Manufacturability for Electric Vehicle: A Review. *Int. J. Sustain. Transp. Technol.* **2022**, *5*, 70–79. [CrossRef]
5. Gibson, L.J.; Ashby, M.F. *Cellular Solids: Structure and Properties*, 2nd ed.; Cambridge Solid State Science Series; Cambridge University Press: Cambridge, UK, 1997; ISBN 978-0-521-49911-8.
6. Costanza, G.; Ferrigno, S.; Tata, M.E. Static compression study of honeycomb panel. *Metall. Ital.* **2021**, *113*, 13–21.
7. Yang, Y.; Liu, H.; Zhang, Q.; Ma, J.; Yang, X.; Yang, J. Energy Absorption Characteristics of a Super Hexagonal Honeycomb under Out-of-Plane Crushing. *Thin-Walled Struct.* **2023**, *189*, 110914. [CrossRef]
8. Fathi, M.; Sameezadeh, M.; Vaseghi, M. Compressive Response and Energy Absorption of Foam-Filled Aluminum Honeycomb Composite: Experiments and Simulation. *J. Braz. Soc. Mech. Sci. Eng.* **2023**, *45*, 562. [CrossRef]
9. Arquilla, G.; Ceci, A.; Costanza, G.; Tata, M.E. Effect of the Load Application Angle on the Compressive Behavior of Al Honeycomb Under Combined Normal–Shear Stress. *Materials* **2023**, *16*, 5462. [CrossRef] [PubMed]
10. Guo, H.; Zhang, J. A Novel Efficient Energy Absorber With Necking-Expansion of Foam Sandwich Tubes. *J. Appl. Mech.* **2023**, *90*, 101012. [CrossRef]
11. Xu, B.; Wang, S.; Yan, W.; Qin, B. A NOVEL EX-Situ Aluminum Foam-Filled Fourfold-Tube Nested System as the Energy Absorber. In Proceedings of the 32nd International Symposium on Ballistics, Reno, NV, USA, 9–13 May 2022. [CrossRef]
12. Peña, A.D.L.; Sato, A.; Latour, M.; Rizzano, G. Conceptual Design of Anti-Seismic Devices with Metal Foam Core for CBFs. *Procedia Struct. Integr.* **2023**, *44*, 2144–2151. [CrossRef]
13. Bhuvanesh, M.; Costanza, G.; Tata, M.E. Research Progress on Mechanical Behavior of Closed-Cell Al Foams Influenced by Different TiH2 and SiC Additions and Correlation Porosity-Mechanical Properties. *Appl. Sci.* **2023**, *13*, 6755. [CrossRef]
14. Costanza, G.; Tata, M.E. Parameters Affecting Energy Absorption in Metal Foams. *Mater. Sci. Forum* **2018**, *941*, 1552–1557. [CrossRef]

15. Wang, Z.; Jing, L.; Ning, J.; Zhao, L. The Structural Response of Clamped Sandwich Beams Subjected to Impact Loading. *Compos. Struct.* **2011**, *93*, 1300–1308. [CrossRef]
16. Radford, D.D.; Fleck, N.A.; Deshpande, V.S. The Response of Clamped Sandwich Beams Subjected to Shock Loading. *Int. J. Impact Eng.* **2006**, *32*, 968–987. [CrossRef]
17. Ryan, S.; Hedman, T.; Christiansen, E.L. Honeycomb vs. Foam: Evaluating Potential Upgrades to ISS Module Shielding. *Acta Astronaut.* **2010**, *67*, 818–825. [CrossRef]
18. Banhart, J. Manufacture, Characterisation and Application of Cellular Metals and Metal Foams. *Prog. Mater. Sci.* **2001**, *46*, 559–632. [CrossRef]
19. Costanza, G.; Montanari, R.; Tata, M.E. Optimisation of TiH_2, and SiC Content in AL Foams. *Metall. Ital.* **2005**, *97*, 41–47.